

Electronic Supplementary Information

Conductive polyaniline-mediated efficient electron transfer in Z-scheme photocatalysts for enhanced overall water splitting

Zhengguo Zhang,^{abc} Guangrong Xie,^{abc} Fang Wang,^{abc} and Shixiong Min^{*abc}

^aSchool of Chemistry and Chemical Engineering, Key Laboratory of Electrochemical Energy Conversion Technology and Application, North Minzu University, Yinchuan, 750021, P. R. China.

^bKey Laboratory of Chemical Engineering and Technology, State Ethnic Affairs Commission, North Minzu University, Yinchuan, 750021, P. R. China.

^cNingxia Key Laboratory of Solar Chemical Conversion Technology, North Minzu University, Yinchuan 750021, P. R. China.

**Corresponding author: sxmin@nun.edu.cn.*

1. Experimental sections

1.1 Chemicals and materials

SrCO_3 , $\text{Rh}_2\text{O}_3 \cdot 5\text{H}_2\text{O}$, $(\text{NH}_4)_2\text{S}_2\text{O}_8$ (APS), and aniline monomer were purchased from Shanghai Titan Scientific Co. Ltd. Aniline was purified twice under reduced pressure and stored below in a refrigerator prior to use. TiO_2 nanoparticles (P25, 20% rutile and 80% anatase) were purchased from Degussa. $\text{Bi}(\text{NO}_3)_3 \cdot 5\text{H}_2\text{O}$ was purchased from Guangzhou Jinhua Chemical Reagent Co., Ltd. Graphene oxide (GO) was purchased from Ashine Advanced Carbon Materials Co., Ltd. All solutions used throughout the experiments were prepared with ultrapure water (18.2 M Ω).

1.2 Preparation of photocatalysts

1.2.1 Preparation of Ru/SrTiO₃:Rh

$\text{SrTiO}_3\text{:Rh}(1\%)$ were synthesized according to a reported procedure.¹ The starting materials of SrCO_3 , TiO_2 , and $\text{Rh}_2\text{O}_3 \cdot 5\text{H}_2\text{O}$ were mixed in a mortar at the ratio of $\text{Sr}:\text{Ti}:\text{Rh}=1.03:0.99:0.01$. The mixture was calcined at 1100 °C for 10 h in air. Ru cocatalyst (1 wt%) that act as an active site for H_2 evolution was loaded on $\text{SrTiO}_3\text{:Rh}$ by photodeposition from an aqueous methanol solution (methanol/water=1/9) containing $\text{RuCl}_3 \cdot 3\text{H}_2\text{O}$. The obtained $\text{Ru/SrTiO}_3\text{:Rh}$ photocatalyst was collected by filtration, washed with water, and dried at 60 °C in a vacuum oven overnight.

1.2.2 Preparation of BiVO₄

BiVO_4 powder was prepared by a liquid-solid reaction.¹ $\text{Bi}(\text{NO}_3)_3 \cdot 5\text{H}_2\text{O}$ (5.33 g) and V_2O_5 (1.00 g) were added into 50 mL of HNO_3 aqueous solution (0.5 M). The suspension was stirred at room temperature for 3 days. The obtained yellow BiVO_4 powder was collected by filtration, washed with water, and dried at 60 °C in a vacuum oven overnight.

1.2.3 Preparation of Ru/SrTiO₃:Rh/PANI/BiVO₄

To synthesize the Ru/SrTiO₃:Rh/PANI/BiVO₄ photocatalysts, Ru/SrTiO₃:Rh and BiVO₄ particles were first dispersed in 20 mL of 1 M H₂SO₄ solution to form a homogenous suspension with a aid of ultrasonication for 30 min. Afterwards, a calculated amount of aniline monomer was added into above suspension and stirred for 30 min to ensure the adsorption of aniline monomer on both of the photocatalyst particles. After that, a calculated amount of (NH₄)₂S₂O₈ (the molar ratio of (NH₄)₂S₂O₈ to aniline was kept to be 1) was dissolved into 5 mL of 1 M H₂SO₄ solution and the obtained solution was added dropwise into above mixture to initiate the oxidative polymerization of the aniline. The polymerization reaction was allowed to proceed for 6 h at 0 °C in an ice bath. The obtained Ru/SrTiO₃:Rh/PANI/BiVO₄ photocatalysts were collected by filtration, washed with water, and dried 60 °C in a vacuum oven overnight.

Ru/SrTiO₃:Rh/PANI and BiVO₄/PANI photocatalysts were synthesized by the identical processes for Ru/SrTiO₃:Rh/PANI/BiVO₄ without the addition of BiVO₄ and SrTiO₃:Rh, respectively. The Ru/SrTiO₃:Rh/BiVO₄ mixture was prepared by filtrating a suspension containing dispersed Ru/SrTiO₃:Rh and BiVO₄ particles. The bare PANI sample without any photocatalyst particles was also prepared using the same experimental procedures.

1.2.4 Preparation of Ru/SrTiO₃:Rh/RGO/BiVO₄ photocatalyst

The Ru/SrTiO₃:Rh/RGO/BiVO₄ photocatalyst was prepared according to a reported procedure.¹ 100 mg of BiVO₄ and 2 mg of graphene oxide (GO) were first dispersed in 50 mL of 50 vol% CH₃OH aqueous solution with the aid of ultrasonication for 2 h. Then, above suspensions were bubbled with N₂ gas and irradiated with a 300-W Xe lamp with a cut-off filter of 420 nm for 2 h, during which the GO was reduced to

RGO by the photogenerated electrons of BiVO₄ to obtain RGO/BiVO₄. Finally, RGO/BiVO₄ was mixed with Ru/SrTiO₃:Rh in water to obtain Ru/SrTiO₃:Rh/RGO/BiVO₄, which was directly used as a Z-scheme photocatalyst for photocatalytic water splitting study.

1.3 Characterization

X-ray diffraction (XRD) patterns were investigated with a Rigaku Smartlab diffractometer with a nickel filtrated Cu K α radiation. Transmission electron microscopy (TEM) and high-resolution TEM (HRTEM) images were taken with a Talos F200x field emission transmission electron microscope. X-ray photoelectron spectroscopy (XPS) measurements of the samples were performed on an ESCALAB Xi⁺ electron spectrometer (Thermo Scientific) using an Al K α X-ray source. Binding energies were referenced to the C 1s peak (set at 284.8 eV) of the sp² hybridized (C=C) carbon from the sample. UV-vis absorption spectra were taken with a Thermo Scientific-Evolution 220 spectrophotometer. Photoluminescence (PL) spectra were determined by a Horiba Scientific FluoroMax-4 spectrofluorometer spectrometer.

1.4 Photocatalytic water splitting reactions

Photocatalytic reactions were performed in a 250 mL reaction cell connected to a closed gas circulation and evacuation system (CEL-SPH2N, CEAULIGHT). A 300-W Xe lamp (CELHXF300) equipped with an optical cut-off filter ($\lambda \geq 420$ nm) was used as light source. In a typical experiment, 100 mg of the photocatalyst was dispersed into 120 mL of water. The pH of the reaction solution was adjusted by using dilute H₂SO₄ solution (0.1 M). Before light irradiation, the reaction system was thoroughly degassed by evacuation in order to remove the oxygen inside the reactor. The reaction solution was continuously stirred and maintained at 6 °C by a flow of

cooling anhydrous ethanol. The amount of evolved H₂ and O₂ gases was determined using an on-line gas chromatograph (CEL-GC-7920, TCD, Ar carrier).

1.5 Photoelectrochemical and electrochemical measurements

All of the electrochemical and photoelectrochemical measurements were performed with an electrochemical analyzer (CS3103, Wuhan Corrtest Instruments Corp., Ltd) in a conventional three-electrode configuration. A Pt mesh (1 cm²) and a Ag/AgCl (in saturated KCl solution) electrode were used as the counter electrode and the reference electrode, respectively. For the photoelectrochemical measurements, the supporting electrolyte was a phosphate buffer (PSB) solution (0.05 M, pH 7) and a 300-W Xe lamp equipped with a cut-off filter of 420 nm was used as a light source. The photocatalyst working electrodes were prepared by electrophoretic deposition on conducting glass supports (FTO) as following: 40 mg of photocatalyst powder and 10 mg of iodine were dispersed in 15 mL of acetone under stirring and sonicated for 10 min. After this process, two FTO electrodes (1 cm×3 cm) were inserted parallel with each other in the above homogeneous suspensions with *ca.* 8 mm of distance, and then 20 V of bias was applied between them for 30 min. After that, the photocatalyst electrodes were dried at 100 °C for 12 h in a vacuum oven. The transient photocurrent response was recorded at a bias of 0.01 V under visible light irradiation. Electrochemical impedance spectroscopy (EIS) was carried out at a forward bias of 0.01 V with an AC amplitude of 5 mV in the frequency range of 10 mHz to 100 kHz under the visible light irradiation. The Mott-Schottky (M-S) measurements were carried out in a 0.5 M Na₂SO₄ (pH 3.5) solution at a frequency of 1 MHz. The cyclic voltammetry (CV) curve of PANI were measured in a 0.5 M Na₂SO₄ solution (pH 3.5) with a scanning rate of 50 mV s⁻¹. The PANI-modified glassy carbon (GC, 3 mm) electrode was prepared as follows: 4 mg of PANI were dispersed in 50 μL of 5

wt% Nafion solution by at least 30 min sonication to form a homogeneous suspension. Then 10 μL of suspension was loaded onto a GC electrode with a loading 0.8 mg cm^2 .

2. Additional figures

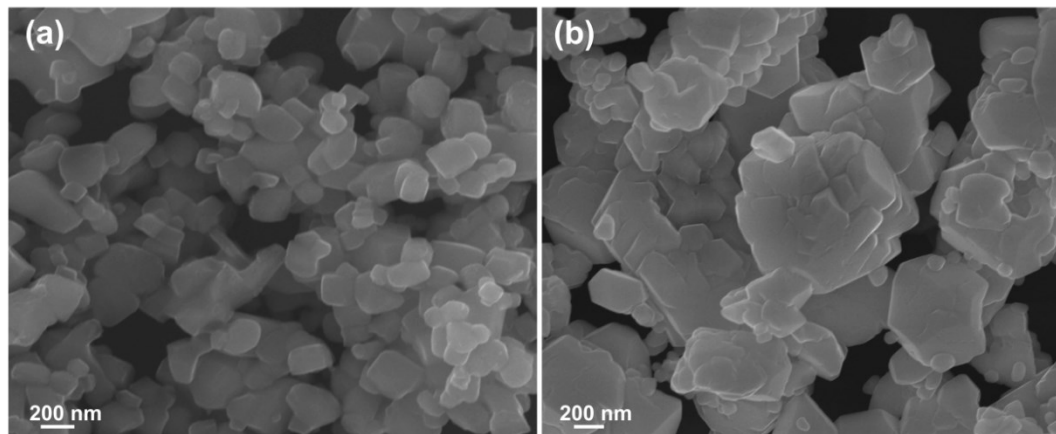


Fig. S1 SEM images of (a) Ru/SrTiO₃:Rh and (b) BiVO₄ particles.

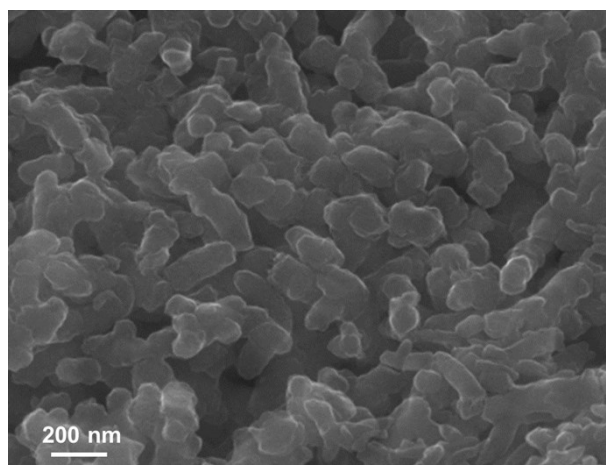


Fig. S2 SEM image of the pristine PANI.

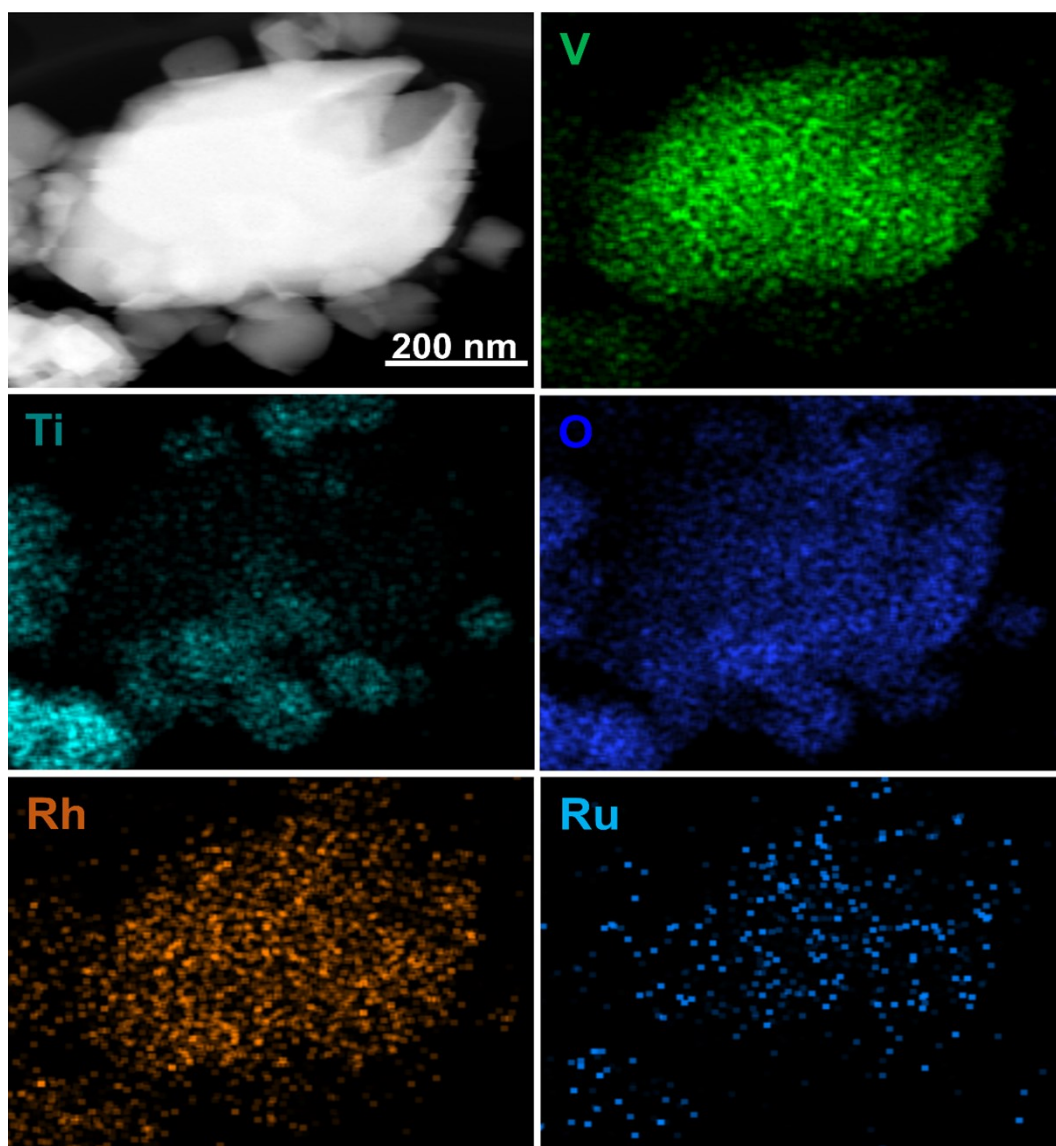


Fig. S3 Additional HAADF-SEM image of Ru/SrTiO₃:Rh/PANI/BiVO₄ and the corresponding EDX elemental maps (V, Ti, O, Rh, and Ru).

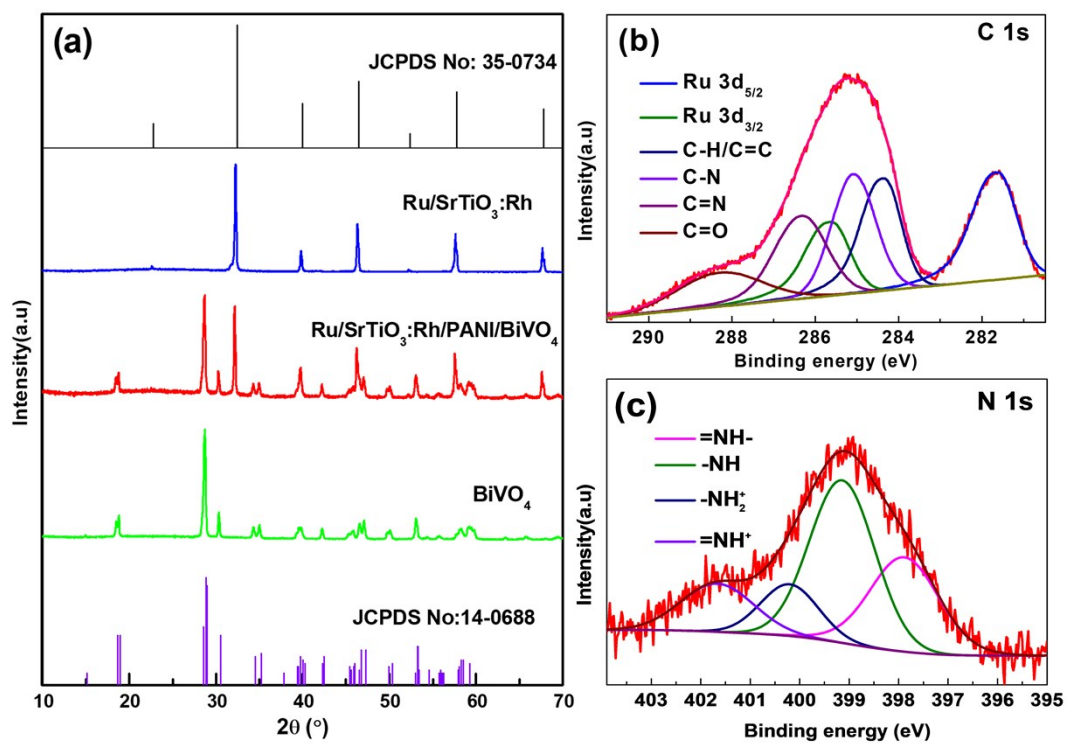


Fig. S4 (a) XRD patterns of Ru/SrTiO₃:Rh, BiVO₄, and Ru/SrTiO₃:Rh/PANI/BiVO₄.

(b) C 1s and (c) N 1s XPS spectra of Ru/SrTiO₃:Rh/PANI/BiVO₄.

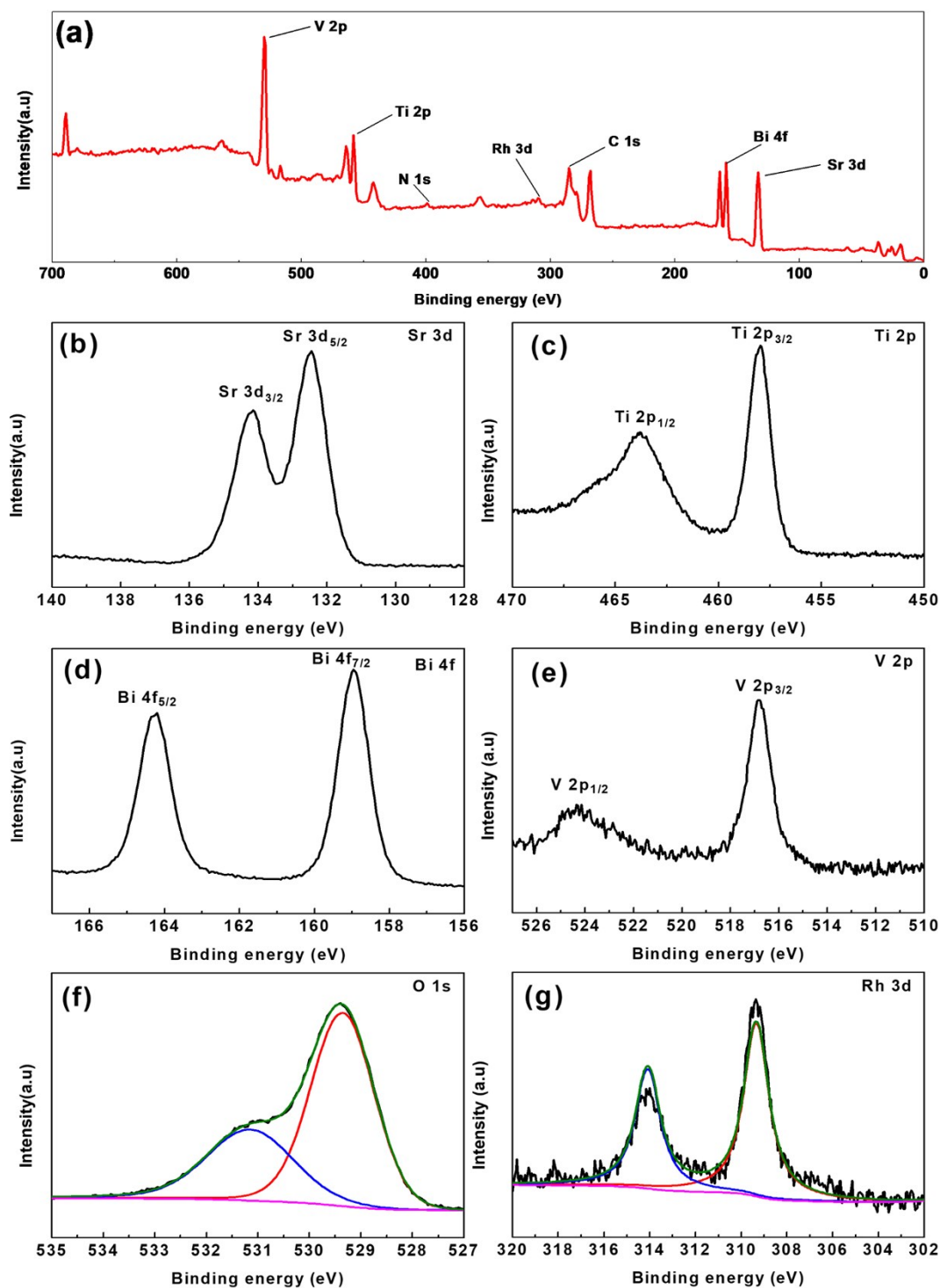


Fig. S5 (a) XPS survey spectrum and (b-g) high-resolution XPS spectra of (b) Sr 3d, (c) Ti 2p, (d) Bi 4f, (e) V 2p, (f) O 1s, and (g) Rh 3d of the Ru/SrTiO₃:Rh/PANI/BiVO₄.

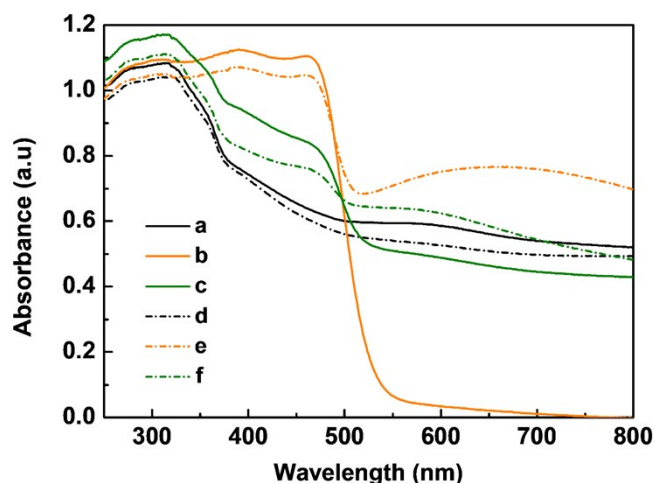


Fig. S6 UV-vis diffuse reflectance spectra (UV-vis-DRS) of (a) Ru/SrTiO₃:Rh, (b) BiVO₄, (c) Ru/SrTiO₃:Rh/BiVO₄, (d) Ru/SrTiO₃:Rh/PANI, (e) BiVO₄/PANI, and (f) Ru/SrTiO₃:Rh/PANI/BiVO₄.

In Fig. S6, it can be observed that the Ru/SrTiO₃:Rh has a steep absorption edge similar to SrTiO₃ at about 390 nm and a broad absorption in the visible light range due to the loading of Ru nanoparticles and the existence of the impurity levels of trivalent Rh species, while BiVO₄ exhibits an excellent absorption towards visible light with an steep edge at around 520 nm. The light absorption spectrum of the physical mixture of Ru/SrTiO₃:Rh and BiVO₄ is the simple sum of two components. After the incorporation of PANI, all of the Ru/SrTiO₃:Rh/PANI, BiVO₄/PANI, and Ru/SrTiO₃:Rh/PANI/BiVO₄ show enhanced light absorption ranging from 520 to 800 nm, which confirm the existence of PANI in the samples.

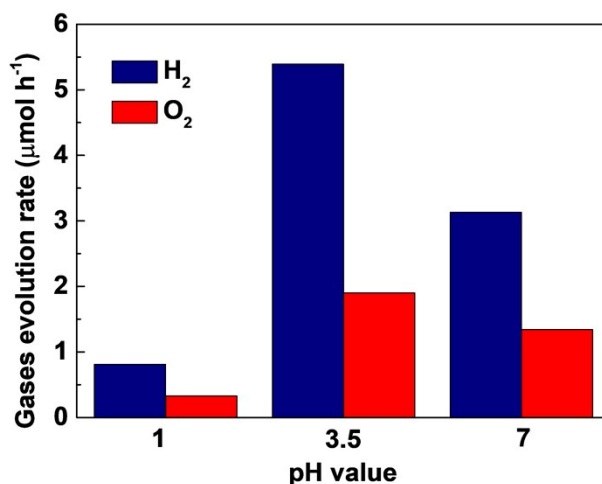


Fig. S7 Effect of the pH value on the H₂ and O₂ evolution activity of Ru/SrTiO₃:Rh/PANI/BiVO₄ catalyst.

It has been previously reported that establishing an intimate physical interaction between the H₂ and O₂ photocatalysts is critical to allow the efficient interparticulate charge transfer and thus greatly improve the photocatalytic activity. In the previous studies, this can be realized by adjusting the pH value of the reaction solution to induce aggregation within the photocatalysts.¹ Similar to the previous findings for bare BiVO₄ and Ru/SrTiO₃:Rh, we also found that our Ru/SrTiO₃:Rh/PANI/BiVO₄ photocatalyst showed the highest activity at pH 3.5 (Fig. S7) probably due to the close assembly of PANI, BiVO₄ and Ru/SrTiO₃:Rh. In addition, as can be seen from Fig. S7, Ru/SrTiO₃:Rh/PANI/BiVO₄ photocatalyst also shows water splitting activity at pH 7, which is lower than the activity obtained at pH 3.5 due to the fact that the H₂ evolution reaction is thermodynamically unfavorable at higher pH values.

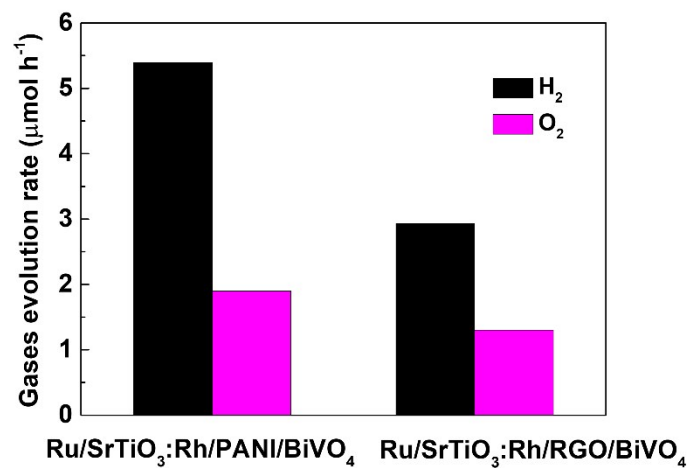


Fig. S8 Photocatalytic water splitting activity of Ru/SrTiO₃:Rh/PANI/BiVO₄ and Ru/SrTiO₃:Rh/RGO/BiVO₄.

Table S1 Comparison of the overall water splitting performance of Z-scheme photocatalysts under visible light irradiation.

Photocatalyst	Photocatalyst dosage (mg)	H ₂ /O ₂ evolution rate (μmol h ⁻¹)	Ref.
Ru/SrTiO ₃ :Rh/RGO/BiVO ₄	30	11/5.5	1
SrTiO ₃ :Rh/np-ITO/BiVO ₄	50	7.5/3.6	2
SrTiO ₃ :La,Rh/Au/BiVO ₄ :Mo	60	48/24	3
Ru/SrTiO ₃ :La,Rh/carbon/BiVO ₄ :Mo	20	8.6/4.4	4
Ru/SrTiO ₃ :Rh/PANI/BiVO ₄	100	5.3/1.9	This work

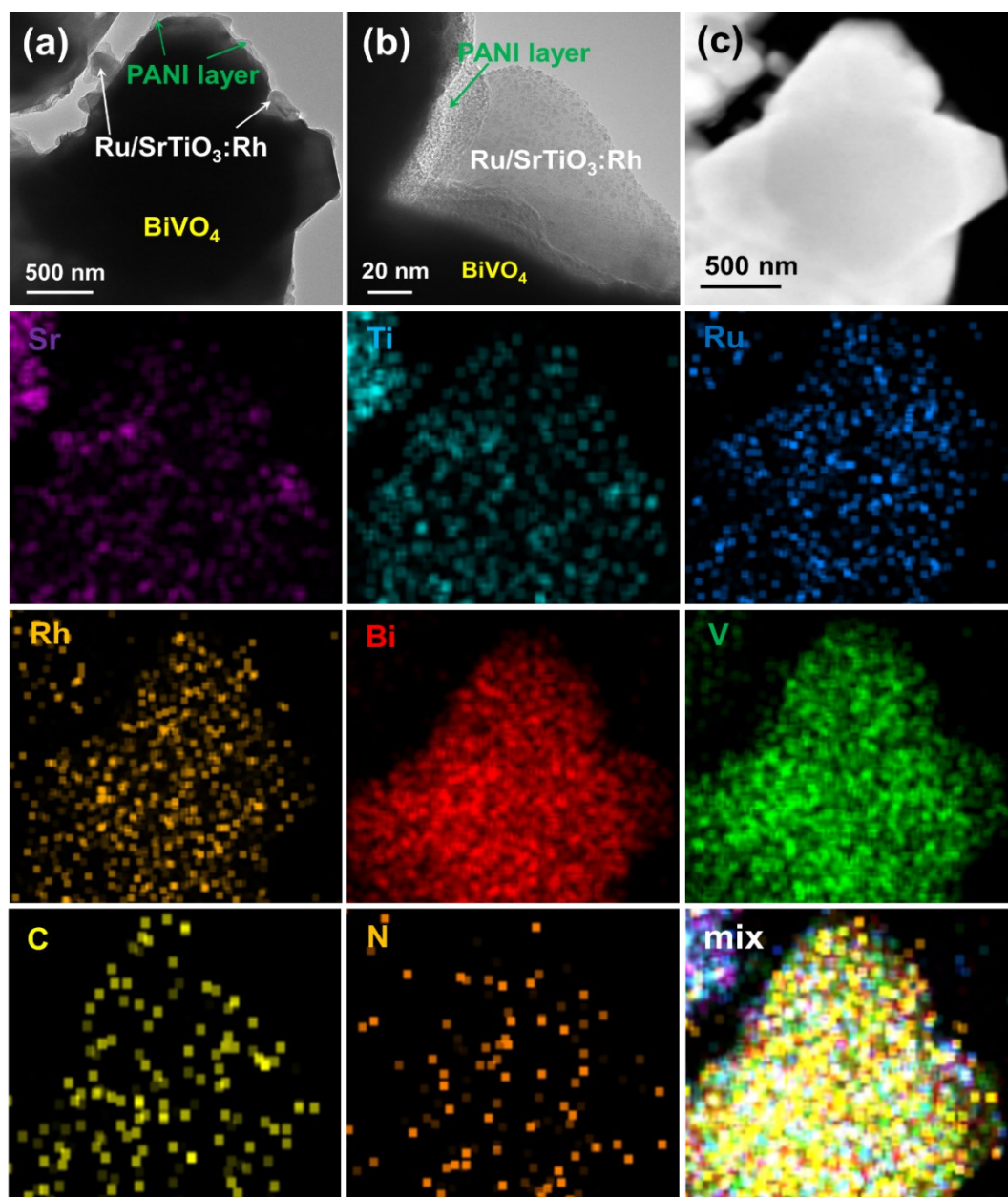


Fig. S9 (a, b) TEM and (c) HAADF-SEM images and the corresponding EDX elemental maps of the Ru/SrTiO₃:Rh/PANI/BiVO₄ after stability test.

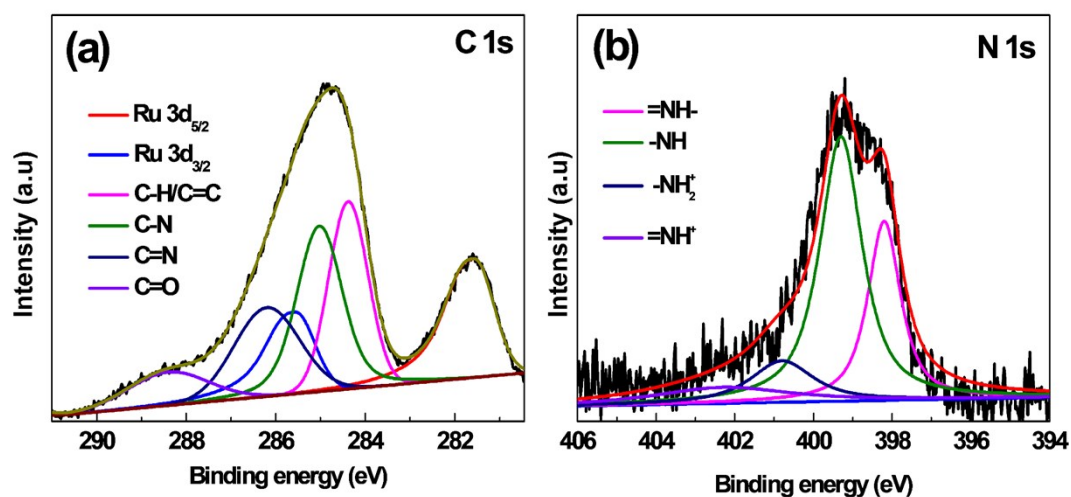


Fig. S10 (a) C 1s and (b) N 1s XPS spectra of the Ru/SrTiO₃:Rh/PANI/BiVO₄ photocatalyst after stability test.

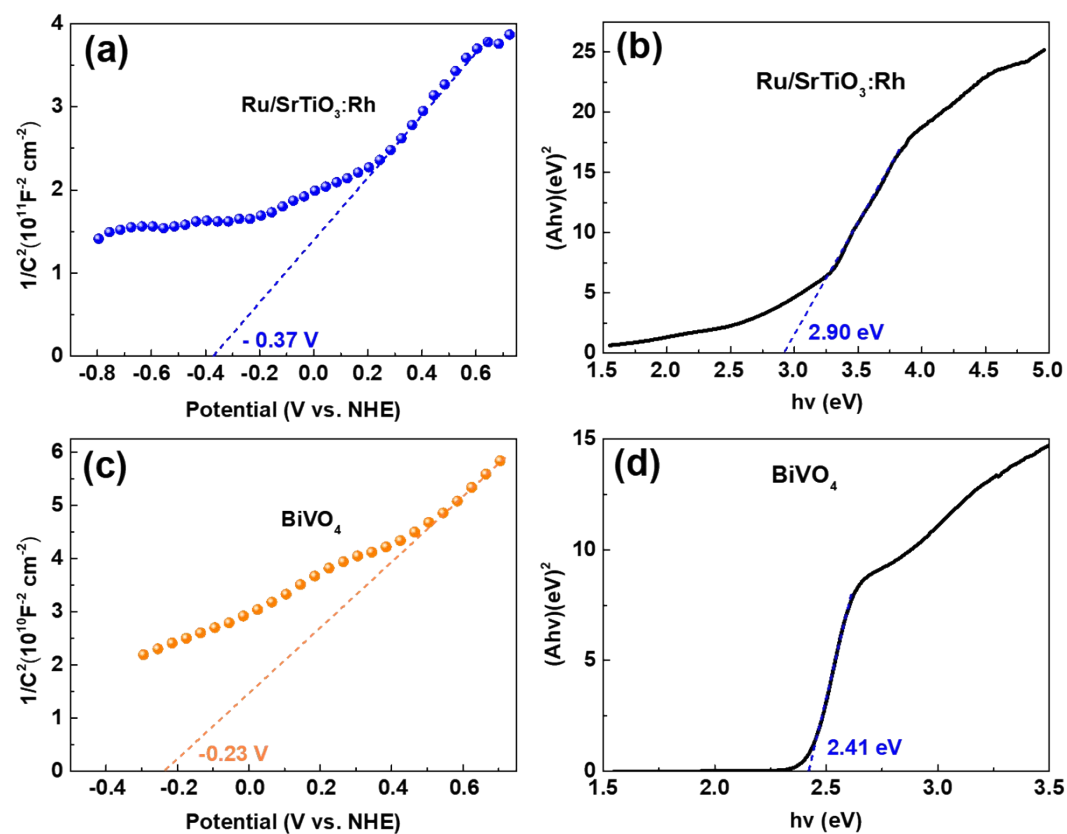


Fig. S11 Mott-Schottky plots of (a) Ru/SrTiO₃:Rh and (c) BiVO₄. Tauc plots of (b) Ru/SrTiO₃:Rh and (d) BiVO₄.

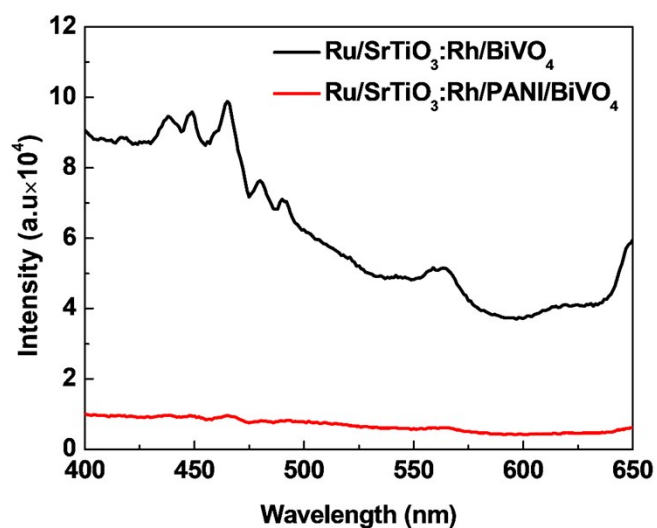


Fig. S12 PL spectra of Ru/SrTiO₃:Rh/BiVO₄ mixture and Ru/SrTiO₃:Rh/PANI/BiVO₄. Excitation wavelength: 340 nm.

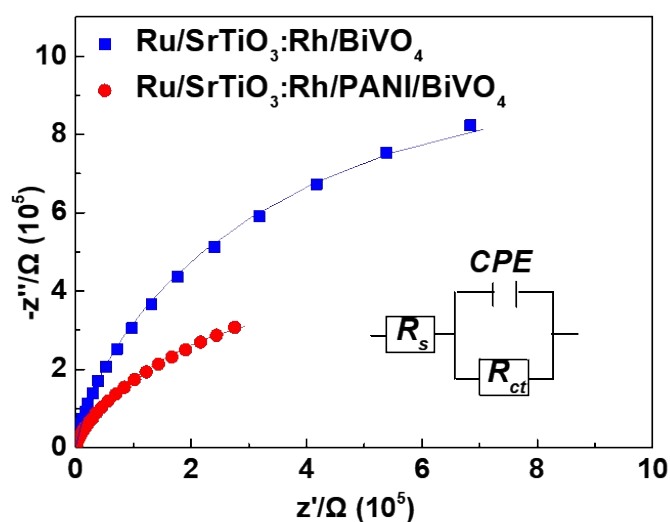


Fig. S13 Electrochemical impedance spectra of Ru/SrTiO₃:Rh/BiVO₄ mixture and Ru/SrTiO₃:Rh/PANI/BiVO₄. The inset is the equivalent circuit for simulating EIS curves.

References

1. A. Iwase, Y. H. Ng, Y. Ishiguro, A. Kudo and R. Amal, *J. Am. Chem. Soc.*, 2011, **133**, 11054-11057.
2. Q. Wang, S. Y. Okunaka, H. Tokudome, T. Hisatomi, M. Nakabayashi, N. Shibata, T. Yamada, K. Domen, *Joule*, 2018, **2**, 2667-2680.

3. Q. Wang, T. Hisatomi, Q.X. Jia, H. Tokudome, M. Zhong, C. Z. Wang, Z. H. Pan, T. Takata, M. Nakabayashi, N. Shibata, Y. Li, I.D. Sharp, A. Kudo, T. Yamada, K. Domen, *Nat. Mater.* 2016, **15**, 611-617.
4. Q. Wang, T. Hisatomi, Y. Suzuki, Z. H. Pan, J. Seo, M. Katayama, T. Minegishi, H. Nishiyama, T. Takata, K. Seki, A. Kudo, T. Yamada and K. Domen, *J. Am. Chem. Soc.* 2017, **139**, 1675–1683.